

Analytical Methods

Accepted Manuscript



This is an *Accepted Manuscript*, which has been through the Royal Society of Chemistry peer review process and has been accepted for publication.

Accepted Manuscripts are published online shortly after acceptance, before technical editing, formatting and proof reading. Using this free service, authors can make their results available to the community, in citable form, before we publish the edited article. We will replace this *Accepted Manuscript* with the edited and formatted *Advance Article* as soon as it is available.

You can find more information about *Accepted Manuscripts* in the [Information for Authors](#).

Please note that technical editing may introduce minor changes to the text and/or graphics, which may alter content. The journal's standard [Terms & Conditions](#) and the [Ethical guidelines](#) still apply. In no event shall the Royal Society of Chemistry be held responsible for any errors or omissions in this *Accepted Manuscript* or any consequences arising from the use of any information it contains.



Journal Name

ARTICLE

Molecularly imprinted electrochemical sensor for advanced diagnosis of alpha-fetoprotein

Received 00th January 20xx,
Accepted 00th January 20xx

DOI: 10.1039/x0xx00000x

www.rsc.org/

Xiaolei Shen, Ya Ma, Qiang Zeng, Jia Tao, Jianzhi Huang, Lishi Wang*

In this work, a low-cost and easily prepared cancer biomarker sensor-alpha-fetoprotein (AFP) biosensor was successfully constructed on the surface of a glassy carbon electrode (GCE) by a surface imprinting procedure using available and cheap agents instead of antibodies. Under optimal detection conditions, the proposed biosensor showed specific recognition ability to free AFP by comparing with other comparative proteins and exhibited a wide linear detection range from 8.0×10^{-4} to $10 \mu\text{g mL}^{-1}$ for AFP with a low detection limit of $9.6 \times 10^{-5} \mu\text{g mL}^{-1}$ (S/N=3). Ultimately, the AFP imprinted sensor was applied to the determination of AFP in human serum sample, giving satisfactory results.

Introduction

Hepatocellular carcinoma (HCC) has recently arisen to the sixth and the third most common cause of general neoplasm and cancer death, respectively. Thus, the early diagnosis and prevention of HCC is turned to be significantly urgent and necessary. Alpha-fetoprotein (AFP), an oncofetal protein with a molecular weight of around 70 kDa, is rarely found in healthy adult organs, but frequently appeared in HCC.¹⁻³ Meanwhile, an increasing number of studies have considered AFP as diagnostic tumor-specific marker for HCC in at-risk patients with the cut-off level of 20 ng mL^{-1} .⁴⁻⁶ This application was firstly described by Abelev⁷ and then AFP was used for the serum diagnosis of primary hepatoma.⁸⁻¹⁰ Totally, for advanced diagnosis and further prevention of liver cancer, alpha-fetoprotein plays a crucial role.

Far to now, there have existed several methods capable of detecting AFP, such as electrophoresis,¹¹ surface plasmon resonance (SPR),¹² colorimetric assay,¹³ enzyme-immunoassay,¹⁴ chemiluminescence,^{15,16} fluorescence methods,¹⁷ enzyme-linked immunosorbent assay,¹⁸ surface enhanced Raman spectroscopy (SERS),¹⁹ and electrochemical immunoassay²⁰ and so on. However, most of these approaches are expensive, time-consuming or requiring highly sophisticated instruments and so on.²¹ Meanwhile, they are antibody-based assays which are the most commonly used diagnostic tool for the analysis of biomolecules.^{22,23} However, antibodies acting as natural recognition material require sophisticated handling and strictly controlled temperature conditions. Duo to their low chemical stability, the applications

of antibody-based assays are limited. Moreover, the affinity between the antibody and its antigen is strong. It's almost impossible to reuse through damaging the binding between the two components after linking.²⁴ Thus, it is necessary to seek for other ways to monitor biomarkers in liver cancer which is expected to bring significant long-term economic, healthy and social benefits to our society.

Currently, on-going research studies have tried to combine molecularly imprinted polymer (MIP) with electrochemical sensors to construct an accurate, low-cost and simple method capable of tracking biomolecules.²⁵⁻²⁷ Because MIP is promising to create artificial receptors by the formation of a polymer network around a template molecule which have robust recognition sites specifically fitting for its print molecule.²⁸⁻³¹ Electrochemical sensors exhibit various excellent properties, such as convenience, low cost, rapidity, good specificity and so on. Their perfect combination must be an attractive and potential approach for the development of biochemical sensors. However, due to the big size, complex structure and conformational fragility of biomacromolecules, this application in biomacromolecules is not as common as in small molecules.

Among all the protein imprinting methods including bulk imprinting, epitope imprinting and surface imprinting, surface imprinting in which a target is imprinted over the surface of its supporter is by far the most successful and popular approach. Based on its advantages of higher binding capability, faster binding kinetics and easy elution than traditional bulk imprinting processes,³² certain success for protein has been achieved by virtue of surface imprinting.³³⁻³⁵ It is worth mentioning that the surface imprinting is particularly suitable for macromolecule imprinting in which diffusion limitation is the major issue.³⁶ Notably, the covalent immobilization of the imprinting molecule on its carrier produces some merits: forming more homogeneous binding sites, impeding template

Key Laboratory of Fuel Cell Technology of Guangdong Province, School of Chemistry and Chemical Engineering, South China University of Technology, Guangzhou 510640, People's Republic of China.
E-mail: wanglsh@scut.edu.cn (L. Wang); Fax: +86 20 87112906

measurements of the AFP-MIP sensor, the electrode was recorded by cyclic voltammetry (CV) from -0.2 to 0.6 V, electrochemical impedance spectroscopy (EIS) performed under its open-circuit potential with the frequency range of 0.1-100 kHz.

The determination of AFP was obtained by differential pulse voltammetry (DPV) measurement which was operated from -0.2 V to 0.6 V with a pulse amplitude of 50 mV. After eluted, the designed electrode was incubated in different concentrations of AFP, then AFP molecules in solution would occupy the imprinted cavities which would prevent $[\text{Fe}(\text{CN})_6]^{3-/4-}$ from arriving at the surface of the prepared electrode leading to the decrease of the current.

We also chose BSA, CEA and HIV-p24 acted as the comparative proteins and NH_4^+ , Na^+ , Ca^{2+} , K^+ , NO_3^- , Cl^- and SO_4^{2-} existing in real sample served as possible interfering ions to evaluate the specific recognition ability of the prepared sensor. All the electrochemical measurements were performed in a PBS buffer solution (pH 7.4) containing 5.0 mmol L^{-1} $[\text{Fe}(\text{CN})_6]^{3-/4-}$ (1:1) and 0.1 mol L^{-1} KCl.

Results and discussion

The principle of the sensor preparation and specific recognition of the AFP

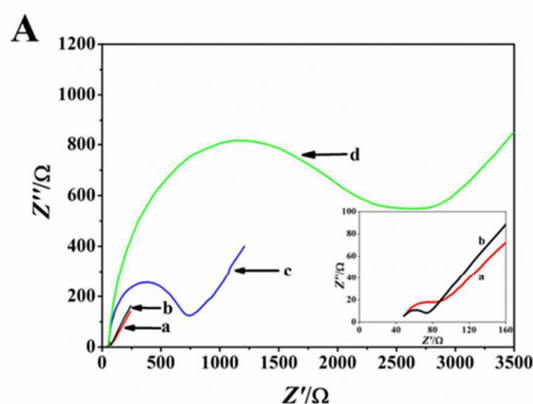
As depicted in Scheme 1, the GCE was abundant with amino-groups by coating a layer of chitosan. Because of the formation of imide group between amino-group on chitosan and aldehyde-group on glutaraldehyde, the glutaraldehyde was bounded to the modified electrode. Based on the similar binding principle, the target molecules were directly covalently grafted on the surface of the resulting electrode. When the AFP bounded electrode was immersed in monomer solution, a large quantity of hydrogen bonds produced by amino and carbonyl bonds of AAm with peptide bond of proteins formed which contributed to the uniform distribution of monomers. Thus, in the presence of cross-linker MBA and the initiator APS, polymerization reaction occurred around the proteins and the templates were well inlaid in the polymer. After eluted with HAc, multiple hydrogen bonds were broken and the target AFP were washed off leaving lots of imprinted cavities only perfectly complementary with the imprinted proteins. When the designed sensor was detected in $[\text{Fe}(\text{CN})_6]^{3-/4-}$ (1:1), a relatively strong DPV signal appeared. However, after the biosensor was immersed in AFP solution, AFP in solution would occupy the imprinted sites based on hydrogen binding interaction and shape memory. Then, a less DPV signal occurred owing to reabsorption of target proteins in the imprinted cavities. Other non-template proteins didn't match the imprinted cavities and were not chemically complementary to the binding sites, thus the AFP-MIP possessed a low absorption capacity to them.

Characterization of the modified electrode

The formation of the proposed AFP-MIP/GA/CS/GCE biosensor had been monitored by both EIS and CV measurements. In particular, EIS was used to reflect the changes of the interfacial property at the GCE surface before and after modification by the charge transfer resistance (R_{ct}) which can be obtained by reading the diameter of the semicircle.⁴⁰ The obtained EIS results were depicted as Nyquist

plots in Fig. 1 (A and C), respectively. Compared with the curve of bare GCE (Fig. 1A, curve a), CS modified GCE showed a relatively smaller R_{ct} value (Fig. 1A, curve b) which can be explained that CS can enhance the electrons transfer rate of the probe. After dropping GA, the resistance slightly increased (Fig. 1A, curve c) due to the hindrance of aldehyde group (-CHO) to the probe. The following introduction of large AFP to the surface of GA/CS/GCE resulted in an increase of the insulating ability of the electrode by hindering interfacial charge transfer between the electrode surface and the electroactive probes in the electrolyte solution, presenting a larger impedance value (Fig. 1A, curve d). By contrast, when the polymeric film was formed on the modified electrode, the resulted impedance (Fig. 1C, curve e) sharply increased from 2500 Ω to almost 1000 Ω due to the further blockage of the insulate imprinted polymer film. However, after eluting AFP from the imprinted film (Fig. 1C, curve f), the impedance of the MIP/GCE obviously decreased because the left AFP cavities allowed more probe to reach the surface of the electrode. After the MIP/GCE electrode was incubated in 1 $\mu\text{g mL}^{-1}$ AFP for 40 min, the impedance became large (Fig. 1C, curve g), suggesting that the template was rebound to the imprinted sites and hindered the diffusion of the probe. In addition, the impedance of curve g was still smaller than that of curve e, indicating that not all of the imprinted sites were occupied.

CV results shown in Fig. 1 (B and D) were consistent with the previous studies of EIS. The binding of AFP (Fig. 1B, curve d) widened the peak-to-peak potential separation and decreased the peak height of $[\text{Fe}(\text{CN})_6]^{3-/4-}$ in the voltammograms, thus leading to the increased R_{ct} value. Meanwhile, the peak-to-peak potential separation of the MIP/GCE before elution (Fig. 1D, curve e) was bigger and the peak height was smaller than the AFP bounded electrode attributing to the insulate film coating on the surface of the electrode. However, when the AFP was removed out of the polymer, an increase of the peak current was observed (Fig. 1D, curve f) because of the formation of imprinted cavities, which left channels for the penetration of probe through the MIP to reach the electrode. After incubating in 1 $\mu\text{g mL}^{-1}$ AFP solution, the imprinted sites were occupied leading to the decrease of the peak current (Fig. 1D, curve g). On the contrary, the EIS and CV curves of the NIP/GCE were nearly overlapped, respectively. This might be attributed to the insulate film and non-formed binding sites which made no evident differences on the NIP electrode surface.



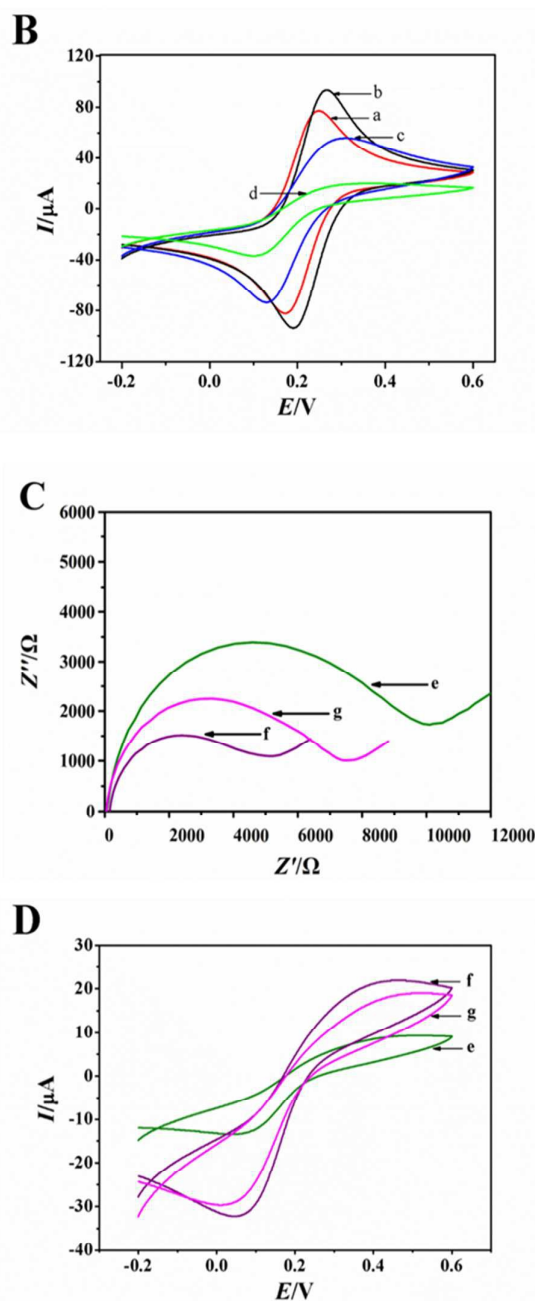


Fig. 1 Electrochemical characterization of the subsequent modification steps of the GCE (a-bare GCE, b-CS/GCE, c-GA/CS/GCE, d-AFP/GA/CS/GCE, e-before removal of AFP from polymeric film, f-after removal of AFP from polymeric film, g-after incubating in $1 \mu\text{g mL}^{-1}$ AFP solution) in a PBS buffer solution (pH 7.4) containing 5.0 mmol L^{-1} $[\text{Fe}(\text{CN})_6]^{3-/4-}$ (1:1) and 0.1 mol L^{-1} KCl, by EIS (A, C, Nyquist plot) and CV (B, D)

Morphological characterizations of AFP-MIP and NIP electrode

Morphologic characterization was taken by SEM. As presented in Fig. 2, obviously significant differences between the imprinted and

the non-imprinted electrode can be observed. The surface of the MIP/GCE was quite rough and porous due to the elution of the target proteins leaving the corresponding cavities (Fig. 2A), on the contrary, the topology of the NIP/GCE (Fig. 2B) is homogeneously wrinkle and condensed because of the formation of the polymer film in the absence of AFP. To a great extent, combining with the EIS and CV results above, we can draw a conclusion that a successful imprinted process had been achieved.

Optimization of experimental condition

The influence of monomer concentration on imprinting capacity was studied by monitoring the change of DPV signal which could indicated the amount of rebinding of AFP. As depicted in Fig. S1 A, with the increase of monomer concentration from 0.4 to 1 mol L^{-1} , the value of ΔI increased and reached the maximum. However, when the concentration exceeded 1 mol L^{-1} , the value of ΔI decreased. This can be explained that for the templates bounded to the prepared electrode, 1 mol L^{-1} AAm could offer enough hydrogen bonds to interact AFP to form stable spatial structure. In this state, the shape, structure and functional groups of the target molecules were completely immobilized by the monomers around them. Too low or too high concentration could not fix the templates well leading to the reduction of binding sites. Thus, 1 mol L^{-1} AAm was used in the following experiments.

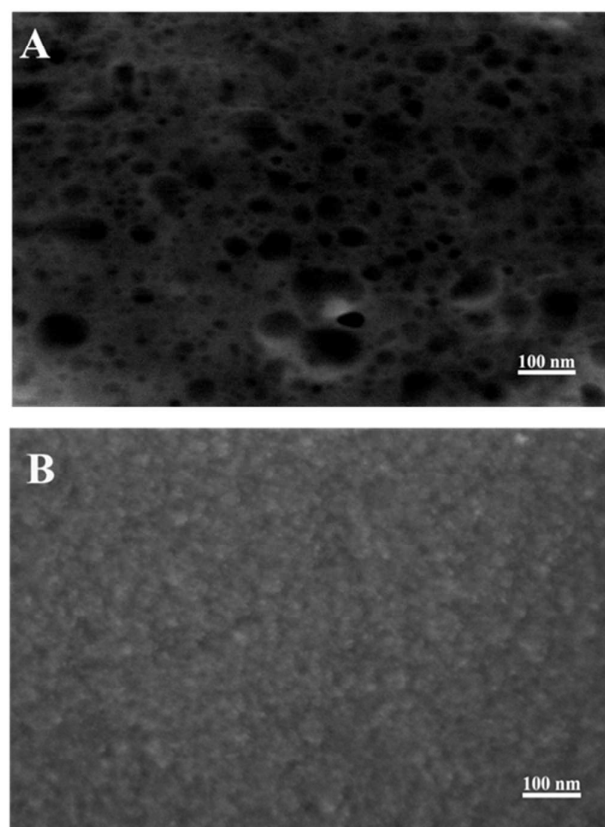


Fig. 2 The SEM images of the MIP/GCE (A) and the NIP/GCE (B).

Cross-linker concentration is another crucial factor affecting adsorption capacity and imprinting efficiency of the proposed sensor. The relationship between crosslinking concentration and ΔI were exhibited in Fig. S1 B. When the crosslinking density was lower than 15 wt.%, the value of ΔI increased with the increase of crosslinking density which could be explained too low crosslinking density was unfavorable to shape and maintain imprinted cavities. In contrast, the value of ΔI declined when the crosslinking density was above 15 wt.%. This trend may be attributed to high cross-linking degree which hindered the targets from entering into the imprinted sites. Therefore, 15 wt.% was adopted as the crosslinking concentration in this assay.

The determination of elution time is a key step for the reconstruction adsorption capacity of the sensor. This performance was measured and optimized by DPV where the variation of the peak current magnitude indicated the amount of removal of AFP. As depicted in Fig. S1 C by the DPV plot, the peak current increased gradually with the elution time and reached the maximum value when the elution time was 6 h. After which time, the peak current was kept indistinguishable, suggesting that AFP had been efficiently removed from the imprinted film. Thus, with the duration of time, the peak current stayed almost unchanged. Therefore, the optimal elution time of 6 h was employed for the construction of the proposed AFP-MIP biosensor.

The readsorption time of the proposed sensor was also studied by DPV (as shown in Fig. S1 D), the peak current decreased with the incubation time until maintaining steady on 40 min. This observation revealed the process of readsorption was made to equilibrium after 40min. Thus, the readsorption time of 40 min was selected in further experiments.

Electrochemical responses of the MIP biosensor to AFP

In this paper, we used the proposed AFP-MIP electrochemical sensor to display the current response to $[\text{Fe}(\text{CN})_6]^{3-/4-}$ by DPV measurement which was much more sensitive than CV. Clear differences were shown between the MIP/GCE and NIP/GCE. The results were depicted in Fig. 3, when the template was removed from the imprinted film, the peak current of the MIP/GCE electrode (Fig. 3A, curve b) increased greatly compared to the electrode before the removal of AFP (Fig. 3A, curve a). This may be explained that the left imprinted sites allowed the penetrating of probe through the polymeric network to contact with the surface of the electrode, thus leading to the higher peak current.⁴¹ Nevertheless, after the MIP/GCE electrode was incubated in $1 \mu\text{g mL}^{-1}$ AFP for 40 min, the peak current decreased clearly (Fig. 3A, curve c), suggesting that the template was rebound to the cavities and hindered the diffusion of the probe. In addition, the peak current of curve c was still larger than that of curve b, indicating that not all of the imprinted sites were occupied. Oppositely, compared with the electrode before the removal of AFP (Fig. 3B, curve a), the peak current of the NIP/GCE electrode after the removal of AFP (Fig. 3B, curve b) increased a little. Meanwhile, an indistinguishable current variation (Fig. 3B, curve c) was observed after the incubation of the NIP/GCE in the AFP solution. All these observations were in accordance with the previous EIS and CV results and suggested that the MIP/GCE electrode can be employed as a proposed sensor for AFP sensing.

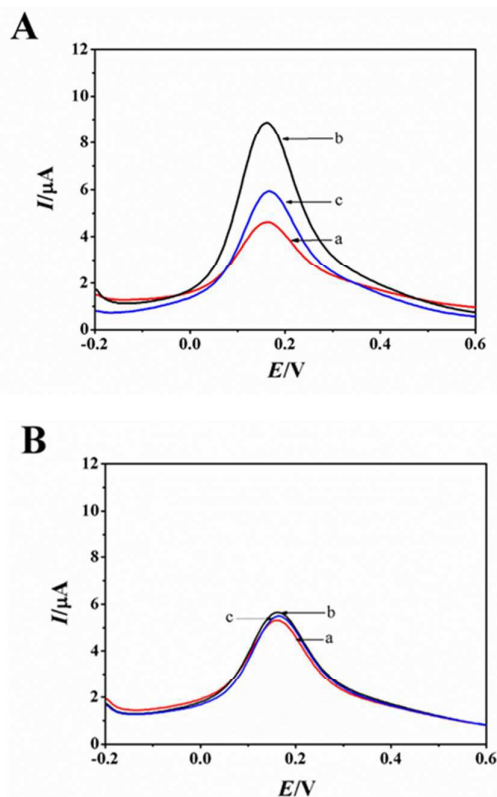


Fig. 3 The DPV plots of MIP/GCE (A) and NIP/GCE (B) performed in PBS buffer (pH 7.4) including $5 \text{ mmol L}^{-1} [\text{Fe}(\text{CN})_6]^{3-/4-}$ (1:1) and $0.1 \text{ mol L}^{-1} \text{ KCl}$: a -before removal of AFP from polymeric film, b -after removal of AFP from polymeric film, c -after incubating in $1 \mu\text{g mL}^{-1}$ AFP solution.

The relationship between the concentrations of AFP and the peak current was demonstrated by DPV under the optimal experimental conditions. As shown in Fig. 4A, accompanying with the increasing AFP concentrations, the DPV peak current of the MIP/GCE decreased gradually. The peak current was found linearly related to the AFP concentration in the range from 8.0×10^{-4} to $10 \mu\text{g mL}^{-1}$ with the regression equation of $I_p (\mu\text{A}) = -0.8524 \text{ Log } c (\mu\text{g mL}^{-1}) + 4.577$ ($R^2=0.992$). The limit of detection (LOD) was obtained as approximately $9.6 \times 10^{-5} \mu\text{g mL}^{-1}$ ($S/N=3$). Comparing with the existed methods (Table S1), we could see each method had its advantages and limitations. However, the developed biosensor was more convenient and possessed a wider linear detection range with a satisfyingly low detection limit which was crucial to the AFP analysis and the biological significance research of AFP in human.

Selectivity

To evaluate the selectivity of the AFP-MIP/GCE, we selected BSA (66.43 kDa), CEA (180 kDa) and HIV-p24 (24 kDa) with different sizes as interfering proteins which can also possibly be found in human serum. The current changes (ΔI) of $[\text{Fe}(\text{CN})_6]^{3-/4-}$ on the MIP/GCE before and after being incubated in the same concentration ($1 \mu\text{g mL}^{-1}$) of each protein were detected by DPV

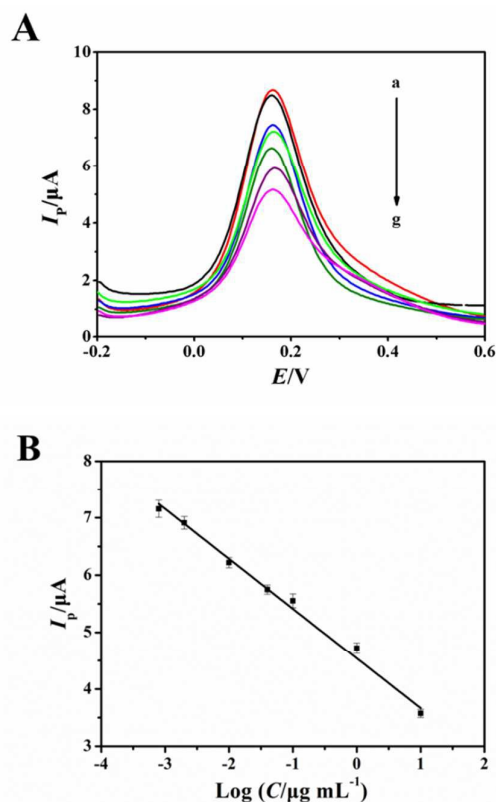


Fig. 4 (A) The DPV curves of MIP/GCE conducted in PBS buffer (pH 7.4) including $5.0 \text{ mmol L}^{-1} [\text{Fe}(\text{CN})_6]^{3-/4-}$ (1:1) and 0.1 mol L^{-1} KCl after rebinding AFP (the concentrations of AFP from a to g were 8×10^{-4} , 2×10^{-3} , 1×10^{-2} , 4×10^{-2} , 1×10^{-1} , 1 and $10 \mu\text{g mL}^{-1}$, respectively). (B) The relative calibration plot of MIP/GCE.

assay and shown in Fig. 5. In particular, the ΔI value of the MIP/GCE electrode toward AFP (66 kDa) was $2.683 \mu\text{A}$, which was 2.8, 5.5 and 9.2 times of that toward BSA, CEA and HIV-p24. As to the structural analogs of BSA, which has a 40.2 % sequence identity and a 59.1 % structural similarity with AFP,⁴² the AFP-imprinted sensor had relatively higher adsorption capacity to another two comparative proteins, but lower adsorption capacity than the target AFP which indicated the predominance of molecular size, shape memory effect and hydrogen interaction mainly affected the imprinting formation and template recognition. However, because of the discrimination between the shape of BSA and the imprinted cavities complementary for AFP and the differences of spatial arrangement of effective groups on the surface of BSA existing, the resulted sensor still possessed some recognition and selectivity to template AFP. As to possible interfering ions such as NH_4^+ , Na^+ , Ca^{2+} , K^+ , NO_3^- , Cl^- , SO_4^{2-} existing in real sample, there was no DPV signal change if they were added or not. In a word, we can confirm that the AFP-imprinted sensor was triumphantly made and had a good selectivity toward its template.

Reproducibility and stability

By analyzing one MIP/GCE biosensor for three times repeatedly, the reproducibility of the AFP imprinted sensor was checked. The relative standard deviation (RSD) was 1.77 %. Afterwards, to fully

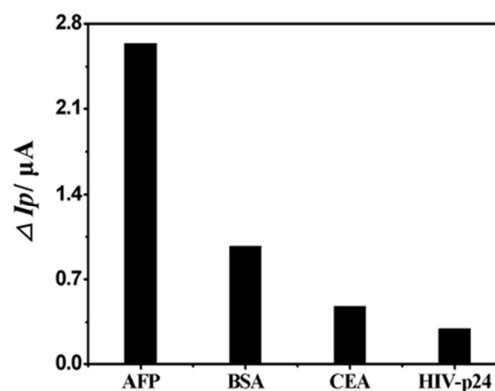


Fig. 5 The peak current variations of the MIP/GCE after being incubated in $1 \mu\text{g mL}^{-1}$ of AFP, BSA, CEA and HIV-p24 solution, respectively.

estimate its reproducibility, we prepared 3 MIP/GCE sensors under the same conditions and used them to detect $1 \mu\text{g mL}^{-1}$ AFP (in PBS). The RSD was 4.26 %. These data indicated that the repeatability and reproducibility of the MIP/GCE sensors were good. As to stability, we measured the peak current variation of AFP-MIP electrode before and after being stored at $4 \text{ }^\circ\text{C}$ for 14 days. The electrodes remained 91% current which confirmed an acceptable stability.

Application assays

To evaluate the application of the determination power of the designed MIP sensor, the standard addition method and high performance liquid chromatography were both applied for determination of AFP. The proposed biosensor was immersed in diluted human serum samples for 40 min which was spiked with different concentrations of AFP. After washed by PBS to remove the physical absorption serum, the sensor was put into $[\text{Fe}(\text{CN})_6]^{3-/4-}$ solution to obtain the DPV signal. The corresponding results shown in Table 1 revealed that the amounts of AFP added and found in the human serum sample existed a satisfying consistency. The recoveries were accounted by the ratio of the detected amount and the added AFP concentration ranging from 96.5 to 107 % with an average relative standard deviation of 3.19 %. Through the statistical comparison between the proposed sensor and the HPLC method, a good agreement at the 95 % confidence level within an acceptable range of error was obtained. Thus, the conclusion that this proposed electrochemical sensor possessed accurate detection property were further confirmed.

Table 1 Results of the recovery experiment

Sample	Added (ng mL ⁻¹)	Proposed MIP sensor			the reference method (HPLC)		
		Found (ng mL ⁻¹ , n=3)	Recovery	RSD (%)	Found (ng mL ⁻¹ , n=3)	Recovery	RSD (%)
1	1.50	1.61	107.0	2.84	1.58	105.3	3.11
2	5.00	5.18	104.0	2.40	5.07	101.4	2.14
3	10.0	9.65	96.5	3.02	9.83	98.3	3.57
4	20.0	19.60	98.0	4.15	19.10	95.5	3.68
5	40.0	40.40	101.0	3.55	39.30	98.3	4.66

Conclusions

An MIP biosensor using biomacromolecule AFP as the sensing target is fabricated on a GCE by a surface imprinting method without any antibody. The modification and imprinting procedure were carefully characterized by CV, EIS, SEM and DPV. Combining advantages of both molecularly imprinting technique and electrochemical methods, the proposed electrochemical AFP-MIP exhibits many outstanding performances, such as low-cost, simple preparation, wide linear range, low detection limit, acceptable stability, specific recognition ability etc., which avail it to be universally applied to clinical disease diagnosis.

Acknowledgements

This work was financially supported by the National Natural Science Foundation of China (Grant Nos. 21475046, 21427809). We also acknowledge the Fundamental Research Funds for the Central Universities (No. 2015ZM050, 2015ZM055 and 2015ZP028).

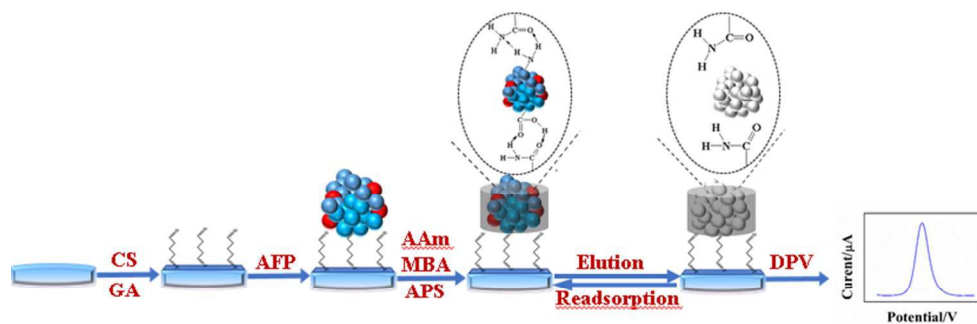
References

- 1 T. Morinaga, M. Sakai, T. G. Wegmann and T. Tamaoki, *Biochemistry*, 1983, **80**, 4604-4608.
- 2 M. Li, S. Zhou, X. H. Liu, P. F. Li, M. McNutt and G. Li, *Cancer Lett*, 2007, **249**, 227-234.
- 3 M. S. Li, H. Li, S. S. Wang, W. Jiang, Z. M. Liu, S. Zhou, X. H. Liu, M. McNutt and G. Li, *Int. J. Cancere*, 2011, **128**, 524-532.
- 4 M. F. Yuen, C. L. Lai, *Best Pract. Res. Cl. Gas.*, 2005, **19**, 91-99.
- 5 T. Malati, *Indian. J. Clin. Biochem.*, 2007, **22**, 17-31.
- 6 F. M. Sanai, S. Sobki, K. I. Bzeizi, S. A. Shaikh, K. Alswat, W. Al-Hamoudi, M. Almadi, F. Al. Saif and A. A. Abdo, *Dig. Dis. Sci.*, 2010, **55**, 3568-3575.
- 7 G. I. Abelev, *Cancer Res.*, 1968, **28**, 1344-1350.
- 8 G. H. Beasall, B. Cook, G. J. S. Rustin and J. Jennings, *Ann. Clin. Biochem.*, 1991, **28**, 5-18.
- 9 H.nOka, A. Tamori, T. Kuroki, K. Kobayashi and S. Yamamoto, *Hepatology*, 1994, **19**, 61-66.
- 10 Y. Aoyagi, Y. Suzuki, M. Isemura, M. Nomoto, C. Sekine, K. Igarashi and F. Ichida, *Cancer*, 1988, **61**, 769-774.
- 11 J. Breborowicz, A. Mackiewicz and D. Breborowicz, *Scand. J. Immunol.*, 1981, **14**, 15-20.
- 12 Y. Teramura and H. Iwata, *Anal. Biochem.*, 2007, **365**, 201-207.
- 13 J. Wang, Y. Cao, Y. Xu and G. Li, *Biosens. Bioelectron.*, 2009, **25**, 532-536.
- 14 Q. Zhang, X. Wang, Z. Li and J. M. Lin, *Anal. Chim. Acta*, 2009, **631**, 212-217.
- 15 X. Wang, Q. Y. Zhang, Z. J. Li, X. T. Ying and J. M. Lin, *Clin. Chim. Acta*, 2008, **393**, 90-94.
- 16 X. Y. Yang, Y. S. Guo, S. Bi and S. S. Zhang, *Biosens. Bioelectron.*, 2009, **24**, 2707-2711.
- 17 X. Xiang, L. Chen, C. Zhang, M. Luo, X. Ji and Z. He, *Analyst*, 2012, **137**, 5586-5591.
- 18 Q. L. Liu, X. H. Yan, X. M. Yin, B. Situ, H. K. Zhou, L. Lin, B. Li, N. Gan and L. Zheng, *Molecules*, 2013, **18**, 12675-12686.
- 19 A. Wang, W. Ruan, W. Song, L. Chen, B. Zhao, Y. M. Jung and X. Wang, *J. Raman. Spectrosc.*, 2013, **44**, 1649-1653.
- 20 D. Wang, N. Gan, H. Z. T. Li, L. Qiao, Y. T. Cao, X. R. Su and S. Jiang, *Biosens. Bioelectron.*, 2015, **65**, 78-82.
- 21 P. Karfa, E. Roy, S. Patra, D. Kumar, R. Madhuri and P. K. Sharma, *Biosens. Bioelectron.*, 2016, **78**, 454-463.
- 22 C. A. K. Borrebaeck, *Immunology Today*, 2000, **21**, 379-382.
- 23 Q. Gao, J. Han and Z. Ma, *Biosens. Bioelectron.*, 2013, **49**, 323-328.
- 24 Tânia S. C. R. Rebelo, C. Santos, J. Costa-Rodrigues, M. H. Fernandes, João P. Noronha and M. Goreti F. Sales, *Electrochim. Acta*, 2014, **132**, 142-150.
- 25 J. P. Li, S. H. Li and C. F. Yang, *Electroanalysis*, 2012, **24**, 2013-2229.
- 26 P. Jolly, V. Tamboli, I. L. Harniman, P. Estrela C. J. Allender and J. L. Bowen, *Biosens. Bioelectron.*, 2016, **75**, 188-195.
- 27 Y. Sun, H. Y. Du, Y. T. Lan, W. J. Wang, Y. J. Liang, C. L. Feng and M. Yang, *Biosens. Bioelectron.*, 2016, **77**, 894-900.
- 28 H. J. Chen, Z. H. Zhang, D. Xie, R. Cai, X. Chen, Y. N. Liu and S. Z. Yao, *Electroanalysis*, 2012, **24**, 2109-2116.
- 29 S. Banerjee and B. Konig, *J. Am. Chem. Soc.*, 2013, **135**, 2967-2970.
- 30 L. X. Sun, D. H. Lin, G. W. Lin, L. Wang and Z. Lin, *Anal. Methods*, 2015, **7**, 10026-10031.
- 31 M. J. Whitcombe, *Nat. Chem.*, 2011, **3**, 657-658.
- 32 F. T. Moreira, S. Sharma, R. A. Dutra, J. P. Noronha, A. E. Cass and M. G. Sales, *Biosens. Bioelectron.*, 2013a, **45**, 237-244.
- 33 H. H. Yang, S. Q. Zhang, F. Tan, Z. X. Zhuang and X. R. Wang, *J. Am. Chem. Soc.*, 2005, **127**, 1378-1379.
- 34 J. Orozco, A. Cortés, G. Cheng, S. Sattayasamitsathit, W. Gao, X. Feng, Y. Shen and J. Wang, *J. Am. Chem. Soc.*, 2013, **135**, 5336-5339.
- 35 J. X. Guo, Y. Z. Wang, Y. J. Liu and Y. G. Zhou, *Anal. Methods*, 2015, **7**, 10018-10025.
- 36 C. J. Tan and Y. W. Tong, *Anal. Bioanal. Chem.*, 2007, **389**, 369-376.
- 37 A. El-Aneel and J. Banoub, *Anticancer Res.*, 2006, **26**, 3293-3300.

ARTICLE

Journal Name

- 1
2
3 38 F. T. C. Moreira, R. A. F. Dutra, J. P. C. Noronha and M. G. F.
4 Sales, *Electrochim. Acta*, 2013c, **107**, 481-487.
5 39 F. Bonini, S. Piletsky, A. P. F. Turner, A. Speghini and A.
6 Bossi, *Biosens. Bioelectron.*, 2007, **22**, 2322-2328.
7 40 Q. Zeng, T. Y. Wei, M. Wang, X. J. Huang, Y. S. Fang and L.
8 S. Wang, *Electrochim. Acta*, 2015, **186**, 465-470.
9 41 J. Luo, S. Jiang and X. Liu, *Sens. Actuators B.*, 2014, **203**,
10 782-789.
11 42 M. H. Lee, A. Ahluwalia, K. M. Hsu, W. T. Chin and H. Y.
12 Lin, *RSC. Adv.*, 2014, **4**, 36990-36995.
13
14
15
16
17
18
19
20
21
22
23
24
25
26
27
28
29
30
31
32
33
34
35
36
37
38
39
40
41
42
43
44
45
46
47
48
49
50
51
52
53
54
55
56
57
58
59
60



Highlights: A biosensor accurate, low-cost and easy preparation is fabricated by a surface imprinting method for specific determination of AFP.

225x105mm (96 x 96 DPI)